

High-precision open-loop adaptive optics system based on LC-SLM

Chao Li,^{1,2} Mingliang Xia,^{1,2} Quanquan Mu,^{1,2} Baoguang Jiang,^{1,2} Li Xuan,¹ and Zhaoliang Cao^{1*}

¹State Key Lab of Applied Optics, Changchun Institute of Optics, Fine Mechanics and Physics, Chinese Academy of Sciences, Changchun, Jilin, 130033, China

²Graduate School of the Chinese Academy of Sciences, Beijing, 100039, China

*Corresponding author: caozlok@yahoo.com.cn

Abstract: Used as a wavefront corrector, a liquid crystal spatial modulator (LC-SLM) has good repeatability and linearity, which are essential for open-loop adaptive optics, and the open-loop optical system can increase the light energy efficiency by a factor of two for the LC-SLM and improve the system bandwidth. In order to test the performance of the LC-SLM in open-loop correction, an indoor closed-loop configuration optical system is constructed on the open-loop control method. With this method, it is demonstrated that the residual error after open-loop correction could be smaller than 0.08λ (RMS: root mean square value) if the initial wavefront aberration is below 2.5λ (RMS), and the repeatability error of open-loop correction is smaller than 0.01λ (RMS).

©2009 Optical Society of America

OCIS codes: (010.1080) Adaptive optics; (230.3702) liquid-crystal device; open-loop control

References and links

1. H. W. Babcock, "The possibility of compensating astronomical seeing," *Publ. Astron. Soc. Pac.* **65**, 229-236 (1953).
2. J. M. Beckers, "Adaptive optics for astronomy: principles, performance, and applications," *Annu. Rev. Astron. Astrophys.* **31**, 13-62 (1993).
3. D. T. Gavel, "Adaptive optics control strategies for extremely large telescopes," *Proc. SPIE* **4494**, 215-220 (2002).
4. J. B. Stewart, A. Dour, Y. Zhou, and T. G. Bifano, "Open-loop control of MEMS deformable mirror for large-amplitude wavefront control," *J. Opt. Soc. Am. A* **24**, 3827-3832 (2007).
5. C. R. Vogel and Q. Yang, "Modeling, simulation, and open-loop control of a continuous facesheet MEMS deformable mirror," *J. Opt. Soc. Am. A* **23**, 1074-1082 (2006).
6. N. Konforti, E. Marom, and S. T. Wu, "Phase-only modulation with twisted nematic liquid crystal spatial light modulation," *Opt. Lett.* **13**, 251-254 (1988).
7. Y. Liu, Z. Cao, D. Li, Q. Mu, L. Hu, X. Lu, and L. Xuan, "Correction for large aberration with phase-only liquid-crystal wavefront corrector," *Opt. Eng.* **45**, 128001 (2006).
8. Q. Mu, Z. Cao, L. Hu, D. Li, and L. Xuan, "Adaptive optics imaging system based on a high-resolution liquid crystal on silicon device," *Opt. Express* **14**, 8013-8018 (2006).
9. S. Serati, X. Xia, O. Mughal, and A. Linnenberger, "High-resolution phase-only spatial light modulators with sub millisecond response," *Proc. SPIE* **5106**, 138-145 (2003).
10. T. Shirai, "Liquid-crystal adaptive optics based on feedback interferometry for high-resolution retinal imaging," *Appl. Opt.* **41**, 4013-4023 (2002).
11. J. Gourlay, G. D. Love, P. M. Birch, R. M. Sharples, and A. Purvis, "A real time closed loop liquid crystal adaptive optics system: first results," *Opt. Commun.* **137**, 17-21 (1997).
12. Q. Mu, Z. Cao, D. Li, L. Hu, and L. Xuan, "Liquid crystal based adaptive optics system to compensate both low and high order aberrations in a model eye," *Opt. Express* **15**, 1946-1953 (2007).
13. D. Cai, N. Ling, and W. Jiang, "Performance of liquid crystal spatial light modulator as a wave-front corrector for atmospheric turbulence compensation," *Proc. SPIE* **6457**, 227-234 (2007).
14. Q. Mu, Z. Cao, C. Li, B. Jiang, L. Hu, and L. Xuan, "Accommodation-based liquid crystal adaptive optics system for large ocular aberration correction," *Opt. Lett.* **33**, 2898-2900 (2008).
15. D. Dayton, J. Gonglewski, S. Restaino, J. Martin, J. Phillips, M. Hartman, P. Kervin, J. Snodgrass, S. Browne, N. Heimann, M. Shilko, R. Pohle, B. Carrion, C. Smith, and D. Thiel, "Demonstration of new

technology MEMS and liquid crystal adaptive optics on bright astronomical objects and satellites,” *Opt. Express* **10**, 1508-1519 (2002).

16. Z. Cao, Q. Mu, L. Hu, D. Li, Z. Peng, Y. Liu, and L. Xuan, “Preliminary use of nematic liquid crystal adaptive optics with a 2.16-meter reflecting telescope,” *Opt. Express* **17**, 2530-2537 (2009).
17. G. D. Love, “Wave-front correction and production of Zernike modes with a liquid-crystal spatial light modulator,” *Appl. Opt.* **36**, 1517-1524 (1997).

1. Introduction

Adaptive optics (AO) was first suggested in astronomy by Backcock for improving the performance of ground-based telescopes [1]. Traditionally a deformable mirror is used as the wavefront corrector. Due to the hysteresis and mechanical coupling between adjacent actuators of the deformable mirror, closed-loop control is generally used to achieve highly accurate wavefront correction [2]. Although closed-loop control is adequate for some AO applications, it is problematic for others, such as extremely large telescopes (ELTs) and multiobject adaptive optics (MOAO) [3]. Besides, the control’s iterative approach limits system bandwidth in an AO system that requires high-speed performance. Thus open-loop control of a deformable mirror is currently being researched [4,5].

The liquid crystal spatial modulator (LC-SLM) has been developed as a wavefront corrector for adaptive optics [6-8], and its good performance has been proved in atmospheric turbulence correction and human eye aberration correction [9-16]. Compared with a deformable mirror, a LC-SLM has a series of attractive characteristics, such as compactness, high density, low cost, low drive voltage, and the possibility of batch production. What’s more, it has good repeatability and linearity, so it will be appropriate for open-loop control adaptive optics.

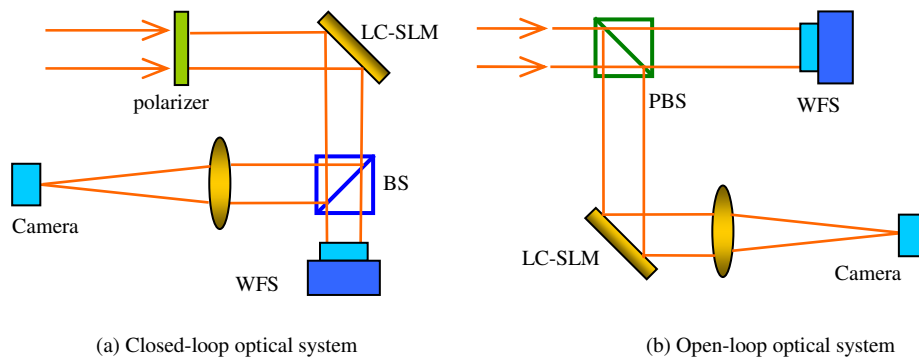


Fig. 1. Sketch of closed-loop and open-loop adaptive optics systems with LC-SLM.

Open-loop adaptive optics systems based on a LC-SLM have the advantage over closed-loop adaptive optics to improve light efficiency by a factor of two. Specifically, a closed-loop SLM-based adaptive optics system requires polarized light. An entrance polarizer cuts half of the light intensity before the LC-SLM. Consecutively, a nonpolarizing beam splitter splits the corrected polarized light between the wavefront sensor and the imaging camera [see Fig. 1(a)]. In contrast, an open-loop adaptive optics system requires a single polarizing beam splitter (PBS). The PBS sends half the light to the wavefront sensor and the other half to the LC-SLM and the imaging camera, fully utilizing the entire light intensity [see Fig. 1(b)]. In addition, an open-loop adaptive optics system requires a single image to capture the LC-SLM control sequence instead of several required by a closed-loop adaptive optics system, therefore increasing bandwidth.

A LC-SLM is proper for open-loop correction, and an open-loop optical system can compensate for the limits of the LC-SLM, so we try to use a LC-SLM in an open-loop

adaptive optics system. In this paper we discuss the performance of a LC-SLM in open-loop correction.

2. Experimental setup and theory

Usually the residual wavefront error after correction is used to evaluate the correction precision for the closed-loop adaptive optics system. But the residual wavefront error could not be measured in the open-loop adaptive system [Fig. 1(b)], so we try to use the open-loop control method on the closed-loop optical system. With this method, open-loop correction is processed, and the correction performance, especially the correction precision, can also be tested. The closed-loop optical configuration is shown in Fig. 2.

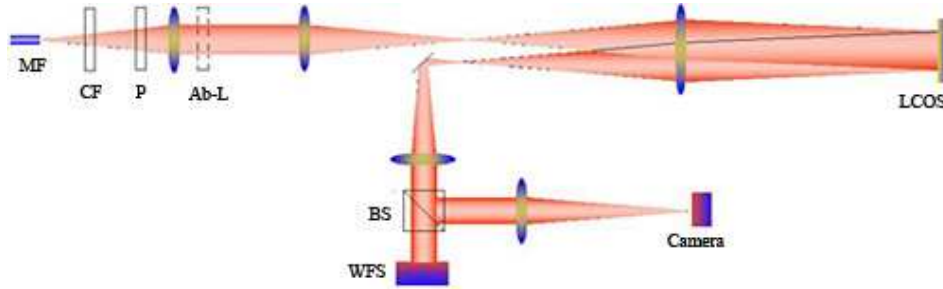


Fig. 2. Layout of the optical system.

The LC-SLM used in the system is a liquid crystal on silicon (LCOS) device produced by BNS Company, and the wavefront sensor is the Shack-Hartmann wavefront sensor (WFS) HASO-32. The light source is a fiber bundle with white light output (MF). The bundle's diameter is 1 mm and its core diameter is 0.025 mm. Due to the chromatic dispersion of liquid crystal, the phase modulation for different colors of light is different, so a color filter (CF, center wavelength of 633 nm and bandwidth of 10 nm) is used to make the light nearly monochromal. A rotatable polarizer (P) is used to polarize the light matching with the LCOS. At the position of Ab-L, which is conjugated with the LCOS, several different aberration lenses can be inserted respectively to induce additional aberration. Behind the corrector LCOS a normal beam splitter is used to split the beam into two parts. One half goes into the imaging camera to form the image, and the other half goes into the WFS (HASO) to measure the residual error. The HASO is also conjugated with the LCOS. The parameters of the HASO and LCOS are listed in Table 1, and the angle between the incident light and the reflected light from the LCOS is 5 deg, so the light is near-normally illuminated. What's more, the half field-of-view angle for the pupil image plane of the LCOS is 0.5 deg.

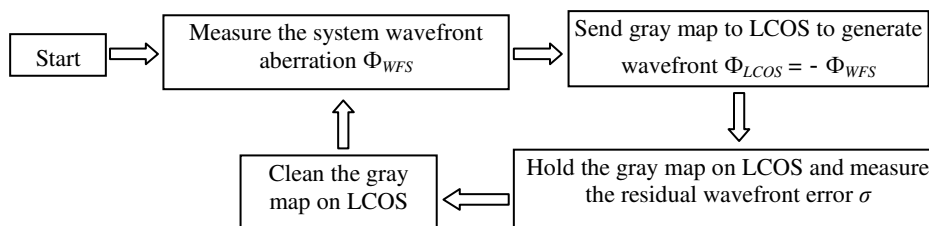
Table. 1. Detailed parameters for the HASO-32 and BNS LCOS

HASO-32		BNS LCOS	
Aperture dimension	4.9 x 4.9 mm	Array size	7.68 x 7.68 mm
Subaperture number	32 x 32	Active pixels	512 x 512
Measurement accuracy in relative mode	1/150 λ (RMS)	Phase levels (resolvable)	50 linear levels for 2π phase stroke
repeatability	< 1/200 λ (RMS)	Response time	7 ms
Working wavelength	450-900 nm	Design wavelength	633 nm
		1st diffraction efficiency	75%

In the typical closed-loop control system, the phase generated by the LCOS can be expressed as

$$\Phi_{LCOS}^i = \Phi_{LCOS}^{i-1} - k \cdot \Phi_{WFS}^i,$$

where Φ_{WFS} is the wavefront tested by the WFS, i is the number of iterations for the closed-loop, and k is the closed-loop proportion factor varying from 0 to 1. In order to process open-loop adaptive correction and measure the residual wavefront error after correction, we use open-loop control theory on the closed-loop optical setup as follows:



It should be emphasized that the systematic wavefront aberration is almost static because the optical system is indoor and compact. Figure 3 shows the wavefront aberration with the system aberration (background) subtracted. The curve in Fig. 3 indicates that the fluctuation of the aberration is smaller than 0.01λ (RMS) in 5 min; therefore the residual wavefront error σ tested in the third step of the correction loop can be considered as the correction error.

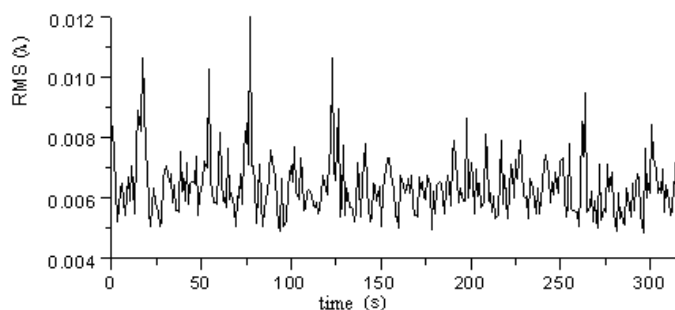


Fig. 3. Wavefront error measured in relative mode for 5 min.

3. Repeatability and linearity of the LC-SLM

In the pure open-loop adaptive optics system, high precision of only one time correction is necessary, because the residual error after correction cannot be detected and recorrected. As a result high wavefront measurement precision for the WFS and high wavefront reconstruction precision for the corrector LC-SLM are necessary. Good repeatability and linearity of the LC-SLM are two key factors to achieve high wavefront reconstruction precision. Due to the high precision of the WFS HASO-32 ($1/150\lambda$ in relative mode), we use it to test the wavefront reconstruction precision of the LC-SLM BNS LCOS first.

The control of the LCOS is based on Zernike polynomials [17], so the precision of wavefront generation for only one Zernike polynomial is tested at first. Figure 4 shows the gray map sent on the LCOS and the wavefront map measured by the WFS when $Z_3=1$ (piston is obviated; Z_0 , x-tilt; Z_1 , y-tilt; Z_2 , defocus, Z_3 , astigmatism; ... Z_{35} . Without remark, $Z_m=j$ means the m th Zernike coefficient is set to j and the other coefficients are set to 0). Figure 5

shows the Zernike coefficients of the reconstructed wavefront measured by the WFS when $Z_2=2$, $Z_3=-2$, and $Z_5=1$. Many more test results are listed in Table 2. The maximum wavefront reconstruction error for the 24 Zernike modals is only 0.046λ RMS.

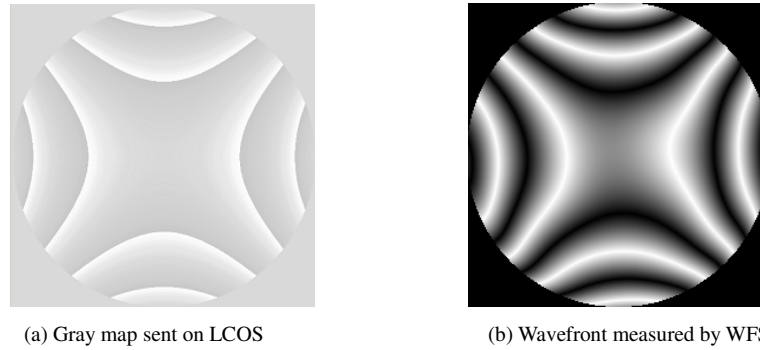


Fig. 4. Wavefront reconstruction test for $Z_3=1$.

Table. 2. Wavefront reconstruction error for Z_4 - Z_{24}

Zernike order	Reconstruction error (RMS)	Zernike order	Reconstruction error (RMS)	Zernike order	Reconstruction error (RMS)
$Z_4=2$	0.034λ	$Z_{11}=1$	0.033λ	$Z_{18}=-2$	0.042λ
$Z_5=1$	0.028λ	$Z_{12}=2$	0.041λ	$Z_{19}=1$	0.031λ
$Z_6=-1$	0.030λ	$Z_{13}=2$	0.037λ	$Z_{20}=1$	0.034λ
$Z_7=-2$	0.041λ	$Z_{14}=1$	0.034λ	$Z_{21}=2$	0.038λ
$Z_8=2$	0.035λ	$Z_{15}=-1$	0.029λ	$Z_{22}=-1$	0.031λ
$Z_9=2$	0.046λ	$Z_{16}=-1$	0.032λ	$Z_{23}=-1$	0.035λ
$Z_{10}=1$	0.038λ	$Z_{17}=2$	0.045λ	$Z_{24}=2$	0.043λ

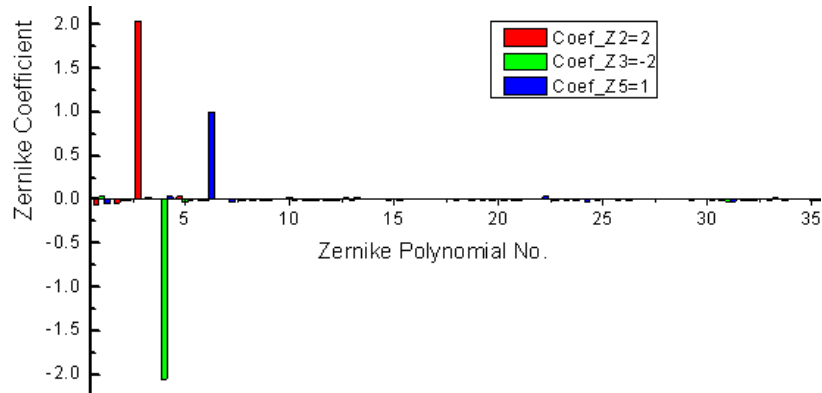


Fig. 5. Zernike coefficient tested by the WFS when the LCOS gray map is $Z_2=2$, $Z_n=0$; $Z_3=-2$, $Z_n=0$; and $Z_5=1$, $Z_n=0$. The reconstruction wavefront error (RMS) is 0.038λ , 0.031λ , and 0.027λ , respectively.

The linearity for LCOS wavefront generation is tested for only Z_2 - Z_7 . Take Z_2 for example; first Z_n ($n=0 \dots 35$ and $n \neq 2$) is set to 0, then Z_2 is set from -3 to 3 in turn, and the reconstructed wavefront is measured by the HASO. The results for the linearity test are shown

in Fig. 6(a). The maximum absolute deviation between the measured Zernike coefficients and the ideal is 0.072, and the maximum relative deviation (normalized by the value of the coefficient) is 5.1%.

The repeatability of the LCOS is tested by this method: the gray map for $Z_m=j$ is sent to the LCOS and cleared repeatedly at 0.25 Hz; the wavefront is tested at 10 Hz simultaneously and the Zernike coefficients of the wavefront are saved. The repeatability test results for Z_2 – Z_7 are shown in Fig. 6(b). The deviations for Z_2 – Z_7 are ± 0.026 , ± 0.043 , ± 0.032 , ± 0.039 , ± 0.045 , and ± 0.051 . Thus the maximum repeatability error is 3.2% relatively.

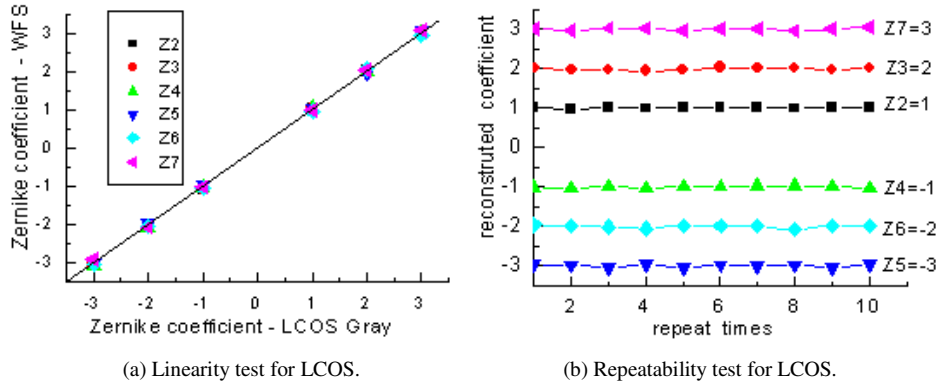


Fig. 6. (a) Linearity and (b) repeatability tests for the LCOS.

As the maximum relative errors for linearity and repeatability are 5.1% and 3.2%, respectively, the maximum possible residual error after correction will be 5%–8% compared with the initial wavefront error. If the initial wavefront error is 1.5λ (RMS), after open-loop correction there will be 0.075 – 0.12λ (RMS) residual error, which can improve the Strehl ratio to 0.57–0.8 at least.

4. Open-loop correction result

The initial system wavefront aberration without any aberration lens inserted at the position Ab-L is about 0.213λ (RMS), and the main component of the aberration is astigmatism, which can be seen from the wavefront map L0 in Fig. 7(a). After correction the residual wavefront aberration is nearly 0.04λ (RMS). Then different eyepieces (myopia eyepiece and astigmatism eyepiece) used as the aberration lens are inserted into the position Ab-L to induce larger aberration. The wavefront maps after the aberration lens is inserted are shown in Fig. 7(a). Figure 7(b) shows the residual wavefront maps after open-loop correction. As the initial aberration increases, the residual aberration after correction increases too. But the residual wavefront error is still smaller than 0.08λ (RMS) even if the initial aberration is larger than 2.5λ (RMS). The peak-to-valley (PV) values of the initial wavefront aberration with L3 and L4 inserted are 9.82λ and 10.13λ , respectively. Simultaneously the image of the fiber bundle is grabbed by the camera, so that we can judge the open-loop correction effect from the image intuitively. It should be emphasized that the ideal resolution at the object space for this optical system is $21.5\ \mu\text{m}$, and the core diameter of the fiber bundle is $25\ \mu\text{m}$.

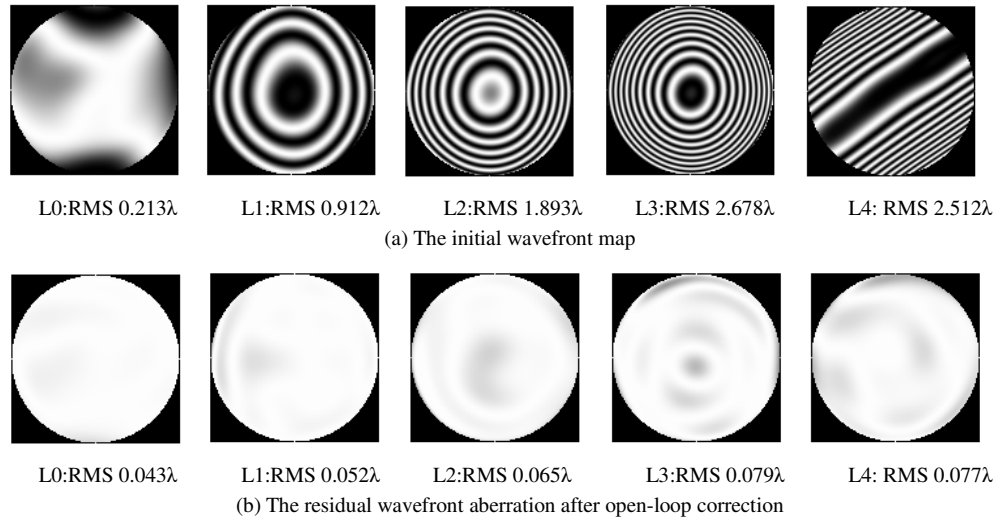


Fig. 7. Wavefront map for different aberration lenses inserted. L0 means no lens inserted, L1 means lens 1 inserted, L2 means lens 2 inserted, and so on. L1–L3 are myopia eyepieces and L4 is the astigmatism eyepiece.

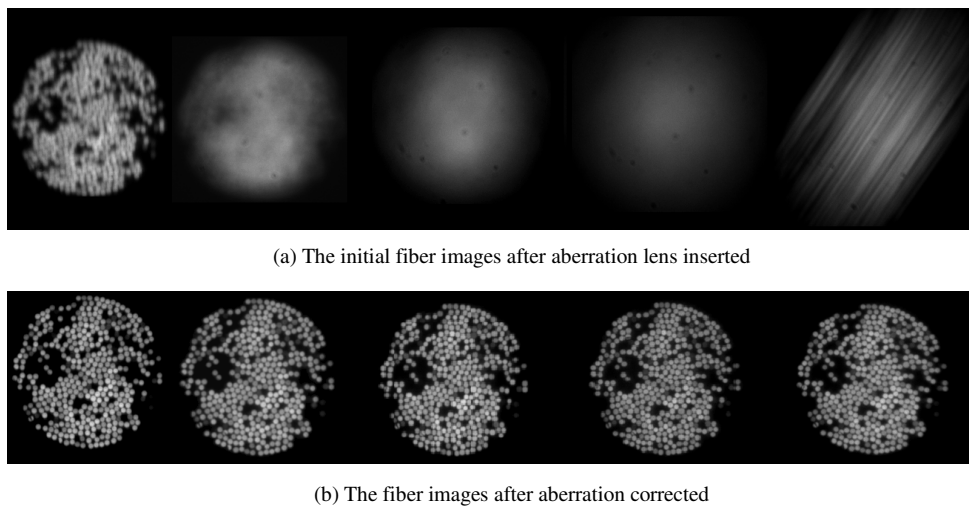


Fig. 8. The fiber images before and after wavefront aberration is corrected. The order for the images is the same as in Fig. 7: from left to right L0 (no lens inserted), L1, ..., L4 in turn.

In addition, the stability is also very important for an adaptive system, so the open-loop correction is repeated for more than 100 cycles for every case (L0–L4) in order to test its stability. The RMS value of the wavefront is calculated during the whole correction process. Figure 9 shows the RMS value of the wavefront for six cycles when lens 2 is inserted and lens 4 is inserted. In each cycle, the wavefront is measured two times before correction and nine times after correction repeatedly. The residual errors after correction vary from 0.060λ to 0.067λ (RMS) during the whole correction process for the case of lens 2 inserted, and the residual errors after correction vary from 0.071λ to 0.079λ (RMS) for the case of lens 4 inserted. It can be concluded from the experimental results that the repeatability precision of the open-loop correction is 0.01λ (RMS).

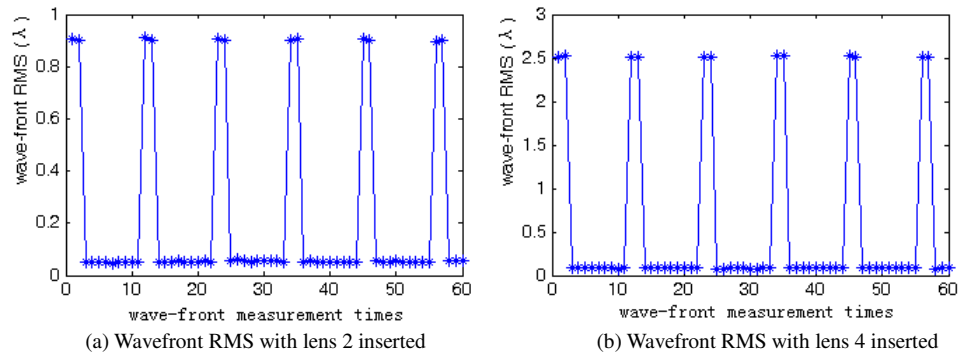


Fig. 9. Wavefront RMS during open-loop correction for about six cycles.

5. Conclusion

A closed-loop adaptive optical system with a Shack-Hartmann wavefront sensor (HASO-32) and a LC-SLM (BNS LCOS) has been constructed based on the theory of open-loop correction. With this method, open-loop correction was carried out and the correction precision was tested. The repeatability and linearity of the LCOS was tested first. Its repeatability error is 3.2% relatively and its linearity deviation is about 5%. In the open-loop correction with the LCOS, the residual error after correction could reach 0.07λ (RMS) when the initial wavefront aberration was below 2λ (RMS), and even if the initial wavefront aberration were larger than 2.5λ (RMS), the residual error after correction could reach 0.08λ (RMS). The repeatability precision of the open-loop correction is 0.01λ (RMS) for the indoor optical system. Besides, by using an open-loop optical system the light energy efficiency for the LC-SLM and the system bandwidth could be improved.

Although a LC-SLM has been used for atmospheric turbulence compensation [15,16], the loss of light energy due to the polarization requirement and the slow response of liquid crystal are the two critical drawbacks. Thus it can be expected that open-loop correction can improve the performance of a LC-SLM for atmospheric turbulence compensation significantly. Besides, the increase of light efficiency will be very beneficial for using a LC-SLM in human eye aberration correction. As the light efficiency increases, the light energy used to illuminate the retina can be reduced, which is much safer for the human eye.

Acknowledgments

This work was supported by National Natural Science Foundation (No. 60578035, No. 50473040, and No. 60736042) and the Science Foundation of Jilin Province (No. 20050520 and No. 20050321-2).